IMTC 2006 – Instrumentation and Measurement
Technology Conference
Sorrento, Italy 24-27 April 2006

A New Calibration Method for Current and Voltage Sensors Used in Power Quality Measurements

Pedro M. Ramos, Nuno B. Brás and A. Cruz Serra
Instituto de Telecomunicações, Department of Electrical and Computer Engineering,
Instituto Superior Técnico, Technical University of Lisbon
Av. Rovisco Pais 1, 1049-001 Lisbon, Portugal
Phone: +351-218418485, Fax:+351-218418472, Email: pedro.ramos@Lx.it.pt

Abstract – *Sensor calibration plays an important role in instrument development and accuracy. This paper presents a method to calibrate current and voltage sensors specially dedicated to power quality measurements which can significantly reduce the distortions introduced by the sensors.*
The first approach to sensor calibration is based on the response of sensors to DC values imposed by a calibrator. The second method is an AC calibration, where a 50 Hz power signal is applied to the sensors also through a calibrator. The calibration coefficients are obtained by minimizing the output distortion. The minimized output distortion is assessed by the signal to noise and distortion ratio (SINAD) at the output of the sensor correction module.

Keywords *– power quality, sensor calibration, sine-fitting.*

I. INTRODUCTION

Nonlinear loads, power utilities deregulation and distributed generation are among the biggest contributors to power quality (PQ) disturbances [1]. The need for power quality assessment has become consumer driven as industry and individual consumers are becoming increasingly aware of the importance of power quality.

Inexpensive, reliable, flexible and accurate power quality instrumentation is based on digital signal processors with powerful algorithms for the detection, classification and measurement of the variety of PQ disturbances. Within these instruments, two very important components are the analog to digital converters (ADC) and the voltage/current sensors.

Sensor calibration is very important since an incorrect calibration can mask some PQ events making them undetectable by the algorithms. The easiest way to implement sensor calibration is by applying a correction polynomial to the acquired samples. This polynomial is also responsible for the required scaling and basically amounts to inverting the transfer functions of the sensors and the ADC.

In this paper, voltage and current close loop Hall effect sensors are calibrated using different methods to estimate the best coefficients for a polynomial correction function of the measured ADC samples.

Different compensation techniques were developed for closed loop Hall Effect transducers to improve linearity [2]. Such techniques can be combined with the proposed calibration method to improve overall sensor linearity. However, the methods developed in [2] are limited to sensors with a hole for the primary winding and are optimized to decrease total harmonic distortion (THD).

II. THE HALL EFFECT SENSORS

The calibration method was developed using a closed loop compensated Hall Effect current transducer (LA 25-NP [3]) and a closed loop compensated Hall Effect voltage transducer (LV 25-P [4]) both from LEM.

According to the manufacturers specifications, the voltage sensor has an overall accuracy of 0.9 %, linearity error below 0.2 %, nominal input voltages up to 500 V RMS, draws a nominal primary current of 10 mA and outputs a nominal current of 25 mA. The output current is fed to a 120 Ω resistor and the voltage drop in this resistor is sampled by a data acquisition board. The current sensor as an overall accuracy of 0.5 %, linearity error below 0.2 % and is configured to operate up to 8 A of nominal current with an output nominal current of 24 mA. The sensor output is also fed to a 120 Ω resistor for current to voltage conversion.

The sensors are assembled in a sensor box, whose basic schematic is presented in Fig. 1. This setup is used to acquire simultaneously the current and the voltage supplied to a specific load.

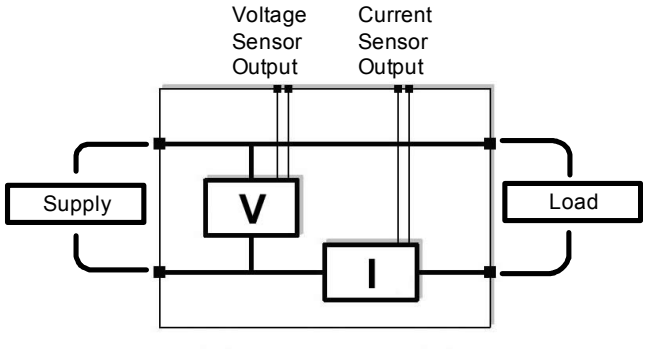

Fig. 1 – Power network sensor box schematic containing current and voltage sensors. The sensor outputs are voltages suitable for direct connection to data acquisition boards.

The sensor box can be used to monitor the current and voltage provided to a load or just to monitor the power grid voltage in a specific access point. In this configuration no load is connected.

III. CALIBRATION MEASUREMENT SETUP

To calibrate the sensor box the experimental setup includes a PC controlled (IEEE 488.2) Wavetek 9100 calibrator. The PC is also equipped with a National Instruments 6013 16-bit data acquisition board (DAQ) to acquire the sensor outputs. The voltage calibration architecture is shown in Fig. 2 while in Fig. 3 the equivalent circuit for current measurement is presented.

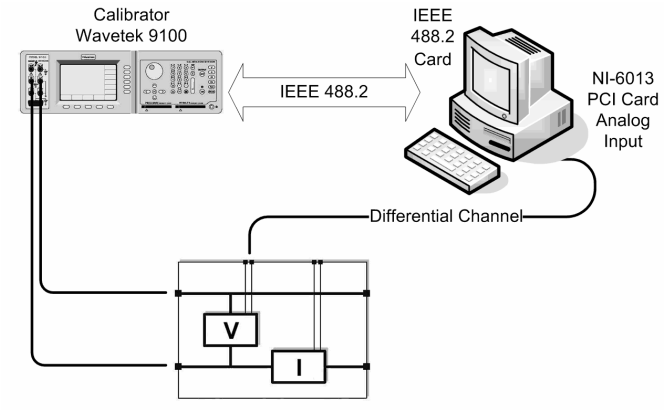

Fig. 2 – Voltage sensor calibration setup.

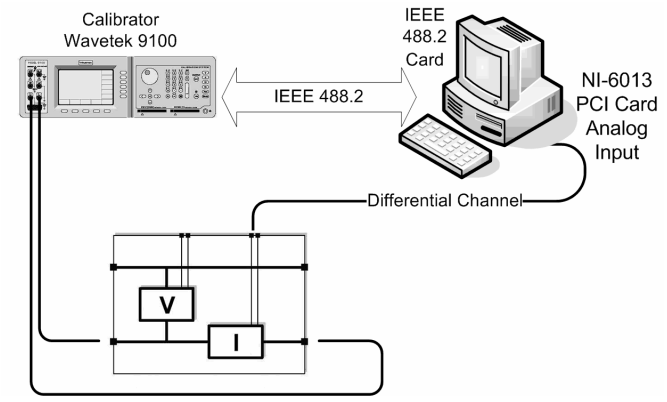

Fig. 3 – Current sensor calibration setup.

A previously developed software platform based on LabVIEW and XML that allows easy acquisition, control of the calibrator and process structured data coming from several acquisitions was used [5].

An analog input signal $x(t)$ is applied to each sensor. The sensor output is then digitized by the DAQ originating the measured values m_i with $i = 1 \ldots N$ where N is the number of acquired samples at relative time instants $t_i = (i-1)/f_S$ (f_S is the DAQ sampling rate).

The digitized record of samples m_i is then fed to a correction module that should output the value of $x(t)$ at instant t_i. This way, the sensor and DAQ transfer functions are inverted in the correction module to obtain an instant estimative of the sensor input signal.

The purpose of the calibration procedure is to find a function $F(m_i)$, to be implemented in the correction module, that minimizes the error between the correction function output $c_i = F(m_i)$ and the sensor input signal at instant t_i.

A schematic representation of the correction procedure applied to the input signal is presented in Fig. 4.

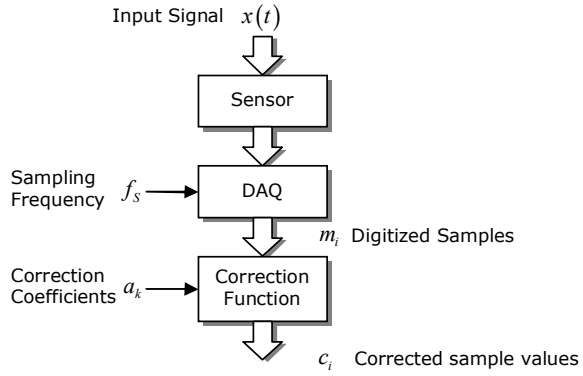

Fig. 4 – Schematic description of a sensor function correction.

The correction function is a polynomial function described by

$$F(x) = \sum_{k=0}^{M} a_k x^k \tag{1}$$

where M is the order of the polynomial function.

This allows good results in the calibration process and is also a simple computational expression which can be easily implemented in DSP based instrumentation.

IV. DC CALIBRATION METHOD

The DC calibration method consists of controlling the calibrator to apply a set of DC voltages to the voltage sensor and determining the a_k coefficients that minimize the distance between the corrected values c_i and the imposed DC voltages in the calibrator. The same technique is also applied to the current sensor where the calibrator now sets the DC current in the sensor box (Fig. 3).

For the voltage sensor, voltages between –400 V and 400 V were applied with the calibrator for a total of 800 different test voltages. This voltage range corresponds to about 52 % of the DAQ range in its ±5 V range.

For each calibrator voltage, 10000 samples were acquired. After the acquisition, the average value was determined together with standard deviation of the acquired samples. A weighted polynomial least-squares fit was applied varying the order of the polynomial fit from $M = 1$ up to $M = 9$.

This process was also performed for the current within the –3 A to 3 A range which accounts for 22 % of the DAC ±5 V range.

The validity of the DC calibration procedure is assessed with a 50 Hz 230 V RMS voltage applied to the voltage sensor. 10 sets of acquisitions each with 10000 samples were executed. The average power spectrum was obtained with the DFT and the SINAD of the corrected values was determined. It should be noted that not all of the ADC range was used, so the determined SINAD should not be used to determine the effective number of bits of the acquisition channel. However, the different values of SINAD obtained with the different order of the polynomial correction function can be used to compare the calibration procedures.

For the current sensor a 50 Hz, 3 A RMS current was used, and the average spectrum was also determined to estimate the SINAD and compare the different order correction polynomial using the DC calibration results.

Fig. 5 shows the SINAD as a function of the polynomial order (M). It can be seen that, for the voltage sensor, there is a steep decrease in the SINAD value for polynomial order above 2. For the current sensor, the SINAD also shows some variation but not as relevant as the change in the voltage sensor.

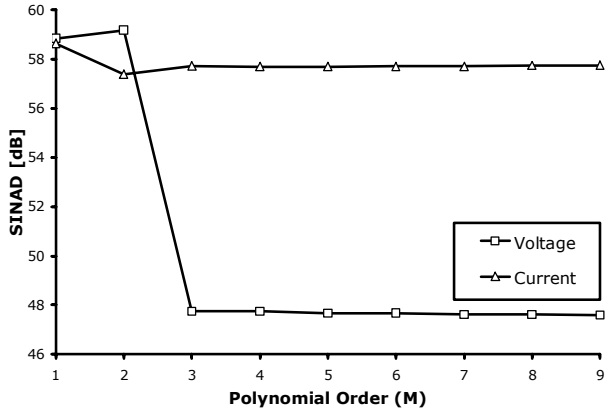

Fig. 5 – SINAD for the current and voltage as a function of the polynomial correction order for DC calibration. The average power spectrum was obtained from 10 sets of 10000 samples. The SINAD was determined from the average power spectrum.

It is clear that the SINAD is not improved when using higher order polynomial correction functions. Since in terms of SINAD, the linear adjustment (polynomial order $M=1$ corresponds to a linear correction) is equivalent to not correcting the harmonic amplitudes, there are no advantages of using higher orders polynomials.

The unimproved SINAD is mostly due to the fact that calibration was performed at DC which doesn't really take into account the distortions that the sensors introduce at 50 Hz. Also, the DC calibration method is not directly intended to improve the SINAD value. It merely adjusts the DC output values to the expected DC input values. However, since the input signal is now a 50 Hz sine signal (either voltage or current), it introduces dynamic behavior to the system (sensor and ADC) that the DC calibration can not take into account.

V. AC CALIBRATION METHOD

To take into account the dynamic behavior of sensors and the fact that the main input signal is a 50 Hz sinewave, a new calibration method was developed and implemented. Instead of using DC values in the calibration step, a sine wave of 50 Hz was applied by the calibrator to the sensors. For the voltage sensor a 230 V RMS was used while 3 A RMS were used for the current sensor.

In this situation, since the input signal is a 50 Hz sine, the corrected values c_i should correspond to the digitized samples of the input signal at the ADC sampling rate. However, there is some information missing that is very important to compare the input signal $x(t)$ with the corrected values c_i. This information is the exact value of the normalized signal frequency (although the calibrator frequency is known with very good accuracy the same does not apply to the DAQ sampling frequency) and the input signal phase. In fact, since the acquisition of samples m_i is not triggered by the actual signal $x(t)$, the initial phase of the samples m_i is a random variable with a uniform distribution. In short, to compare the record c_i with the samples of $x(t)$ sampled at f_S, the exact signal frequency of $x(t)$ and the phase corresponding to the first sample must be determined. To achieve this objective, a four-parameter sine-fitting [6] is used to estimate the phase (ϕ) and the frequency (f) of the corrected values c_i. Afterwards a virtual version of the input signal is now available

$$\hat{x}(t) = A_{RMS}\sqrt{2}\cos(2\pi f t + \phi) \tag{2}$$

where A_{RMS} is calibrator imposed value (230 V for the voltage and 3 A for the current). The polynomial correction function can be assessed by comparing the corrected samples c_i with the sampled record of (2) at the sampling rate f_S

$$\hat{x}_i = \hat{x}\left(t = \frac{i-1}{f_S}\right) = A_{ef}\sqrt{2}\cos\left[2\pi\frac{f}{f_S}(i-1)+\phi\right]. \tag{3}$$

To compare the records c_i and $\hat{x}_i$, the sum of the squared errors can be used

$$\varepsilon = \sum_{i=1}^{N}(\hat{x}_i - c_i)^2 . \tag{4}$$

This cost function amounts to quantify the distance between the corrected record c_i and the input sine signal. The correction procedure determines the correction function coefficients a_k that minimizes (4), which is the same as maximizing the SINAD of c_i.

The optimization problem that leads to the best set of polynomial coefficients can be represented by

$$\varepsilon(a_0,...,a_M) = \min_{a_k}\left[\sum_{i=1}^{N}(\hat{x}_i - c_i)^2\right] \quad (5)$$

where $c_i = F(m_i)$.

The proposed optimization algorithm can be defined with the pseudocode

Algorithm

Input:

- → Acquired sensor samples (m_i) and timestamps, (t_i)
- → Initial estimation of polynomial coefficients (a_k) for function $F(x)$

Output:

- → Coefficients (a_k) that minimize the cost function ε

Body:

SET iter to 0

REPEAT

INCREMENT iter

CALCULATE $c_i = F(m_i)$

CALL SINEFIT with t_i, c_i RETURNING ϕ and f

CALCULATE $\hat{x}_i = A_{ef}\sqrt{2}\cos\left[2\pi\frac{f}{f_S}(i-1)+\phi\right]$

CALCULATE $\varepsilon = \sum_{i=1}^{N}(\hat{x}_i - c_i)^2$

SOLVE $\min_{a_k}(\varepsilon)$ RETURNING new coefficients a_k

UNTIL (Δε<εresol OR ε<εmin OR iter>MaxIter)

In this algorithm, εmin is a fixed threshold for the cost function. When ε<εmin the algorithm stops because it has achieved the desired cost function value. εresol is the desired resolution for the cost function. When the algorithm fails to improve above εresol, the algorithm stops because it has converged. The algorithm stops when the number of iterations exceeds MaxIter.

Convergence depends on the initial a_k correction coefficients. Our experience shows that, by choosing the DC calibration coefficients as the initial estimates, convergence is assured.

A. SINAD Analysis

In this section the average power spectrums of 10 sets of acquisitions before and after calibration are presented. The results were obtained with 99001 samples per set (adjusted to reduce spectral leakage) acquired at 50 kS/s. In Fig. 6 the normalized average power spectrum of the acquired samples c_i is shown. Cleary present are several signal harmonics, namely the second, third and many more. The SINAD value is 60.1 dB.

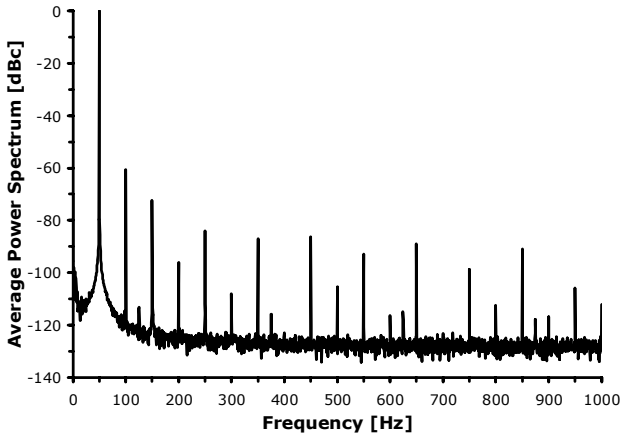

Fig. 6 – Voltage sensor normalized average spectrum, obtained with 10 sets of 99001 samples each, acquired at 50 kS/s for a 50 Hz signal before correction.

The corrected normalized average power spectrum is shown in Fig. 7 for the ninth order polynomial correction function. These results were obtained from the uncorrected samples of Fig. 6. The first few harmonics with higher amplitudes of Fig. 6 now have much reducer amplitudes demonstrating the usefulness of the proposed correction method. The SINAD value after correction is 74.9 dB, which is an improvement of 14.8 dB (the equivalent of an increase in the number of effective bits of 2.46).

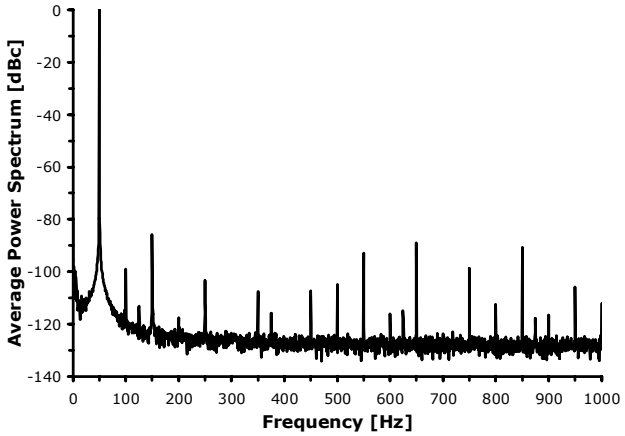

Fig. 7 – Corrected voltage sensor normalized average spectrum, obtained with 10 sets of 99001 samples each, acquired at 50 kS/s for a 50 Hz signal after correction with 9th order polynomial function.

Also note that, the higher harmonics have their amplitude unchanged. This can be explained by the analysis of the natural powers of a sine signal [7]

$$\left[\cos(x)\right]^{2n} = \frac{1}{2^{2n}}\binom{2n}{n} + \frac{1}{2^{2n-1}}\sum_{k=0}^{n-1}\binom{2n}{k}\cos\left[2(n-k)x\right], \quad (6)$$

$$\left[\cos(x)\right]^{2n+1} = \frac{1}{4^{n}}\sum_{k=0}^{n}\binom{2n+1}{k}\cos\left[(2n+1-2k)x\right]. \quad (7)$$

This means that for example the 9th power can introduce frequency corrections at f, $3f$, $5f$, $7f$ and $9f$. Since the power of the correction polynomial is limited to 9, only harmonics up the 9th can be corrected.

In Fig. 8, the normalized average power spectrum for the current is shown while the corrected spectrum is shown in Fig. 9. The SINAD improves from 59.7 dB up to 68.4 dB.

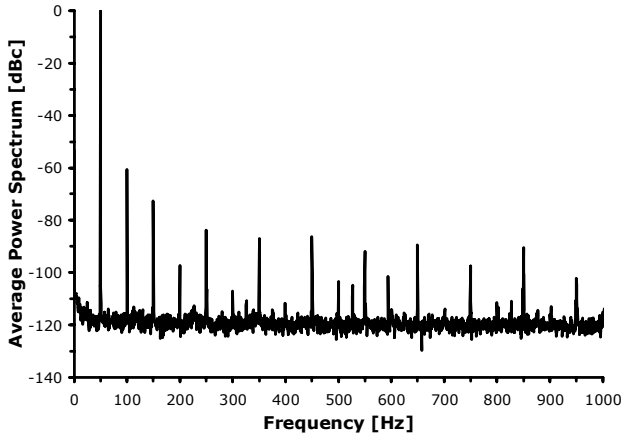

Fig. 8 – Voltage sensor normalized average spectrum, obtained with 10 sets of 99001 samples each, acquired at 50 kS/s for a 50 Hz signal before correction.

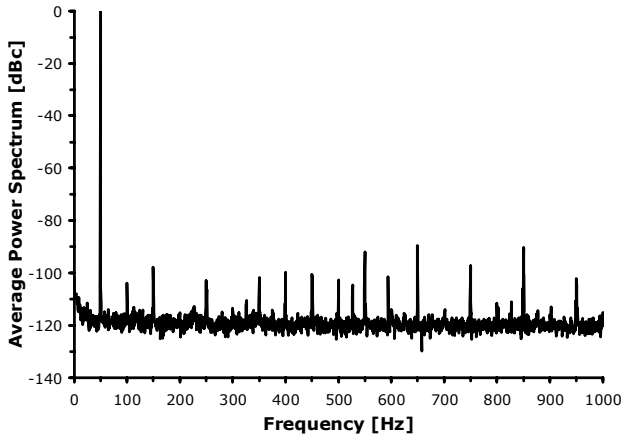

Fig. 9 – Corrected current sensor normalized average spectrum, obtained with 10 sets of 99001 samples each, acquired at 50 kS/s for a 50 Hz signal after correction with 9th order polynomial function.

To quantify the improvements, the SINAD as a function of the polynomial order was calculated and is shown in Fig. 10, for both current and voltage sensors calibration.

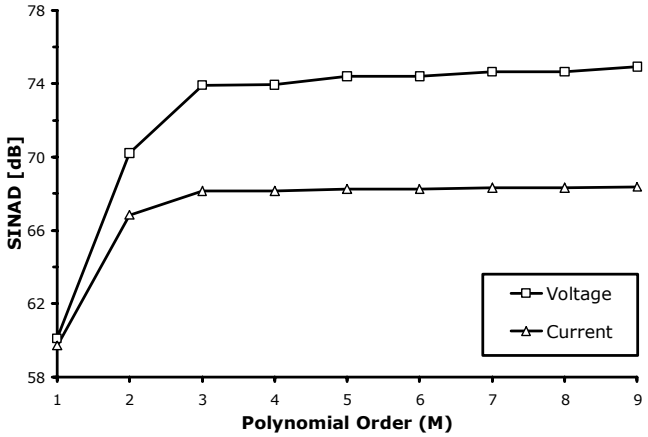

Fig. 10 – SINAD value of the corrected sample values as a function of the polynomial degree of calibration.

Contrarily to what happened in the DC calibration, there is a considerable improvement in terms of SINAD. The difference between the improvements obtained in current and voltage can be consequence of the different DAQ input voltage range used in each case (42% for voltage and 30% for current) or different sensor distortion at 50 Hz.

In Table I the correction coefficients for the voltage and current sensor obtained with the AC calibration method are presented.

Table I. Correction coefficients for the voltage and current sensor obtained the AC calibration method.

Polynomial Coefficient	Voltage sensor	Current Sensor
a_0	0.25939 V	-0.00523 A
a_1	154.94905	2.77857 A/V
a_2	-0.13760 V^{-1}	-0.00386 A/V^2
a_3	-0.36503 V^{-2}	-0.01199 A/V^3
a_4	-0.00385 V^{-3}	0.00092 A/V^4
a_5	0.20956 V^{-4}	0.01285 A/V^5
a_6	0.00158 V^{-5}	-0.00065 A/V^6
a_7	-0.05362 V^{-6}	-0.00618 A/V^7
a_8	-0.00013 V^{-7}	0.00015 A/V^8
a_9	0.00486 V^{-8}	0.00105 A/V^9

B. Frequency Response Analysis

To assess the frequency response of the voltage sensor, a different setup is used. Two Wavetek 9100 are connected in series as shown in Fig. 11. With this setup it is possible to add a spurious frequency to the larger signal whose frequencies and amplitudes can be independently changed. The setup is also useful to test real power quality measurement situations, where a small amplitude spurious harmonic affects the power signal.

The small amplitude spurious signal can also be directly measured by a third differential channel of the data acquisition board.

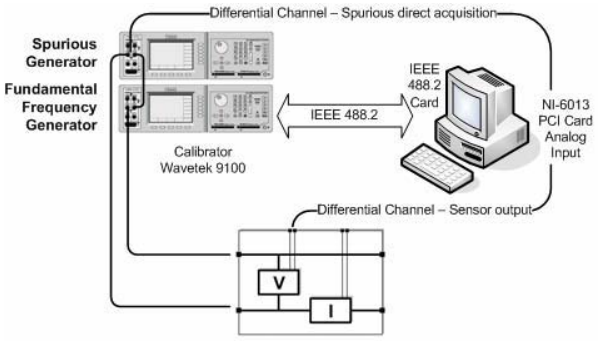

Fig. 11 – Setup to measure the voltage sensor response to smaller amplitude spurious voltages with independent control of both signals.

Preliminary results of the assessment of the voltage sensor include: (i) frequency response of the sensor to the large power signal and (ii) frequency response of the sensor to the smaller spurious signal.

In Fig. 12 the response of the voltage sensor to the large signal frequency variations is shown. Up to 30 kHz (which is the frequency limit of the calibrator), the frequency response of the sensor introduces only a maximum loss of 2 dB.

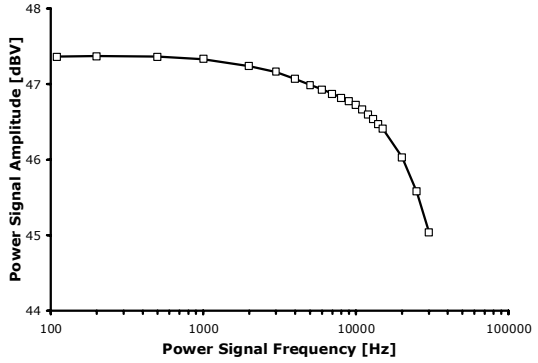

Fig. 12 – Frequency response of the power signal amplitude without spurious component.

The frequency response of the sensor to the spurious signal frequency was determined with a 230 V, 50 Hz power signal and a 2.3 V spurious frequency signal. In Fig. 13 the measured spurious signal amplitude is shown as a function of the spurious frequency.

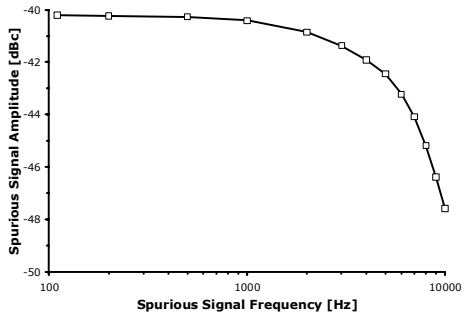

Fig. 13 – Frequency response of the spurious signal with 2.3 V. The power signal has 230 V at 50 Hz.

Clearly, the bandwidth for the spurious signal is much smaller than the bandwidth of the power signal (Fig. 12). This may be caused by the presence of the larger power signal.

VI. CONCLUSIONS

A method for AC calibration of power quality sensors has been presented. It can improve the measured SINAD by 14.8 dB for the voltage sensor and 8.7 dB for the current sensor, using a ninth order polynomial correction function.

The sensors bandwidth has been assessed with a setup that allows the addition of a variable amplitude and frequency spurious signal.

Further improvements require a more precise knowledge of the calibrator actual imposed signal to the sensors. In fact, the calibrators own THD is affecting the results since the calibrating procedure is also trying to correct the input signal THD. However, with the spectral composition of the input signal, spectral correction techniques must be used.

ACKNOWLEDGMENTS

Work sponsored by the Portuguese national research project reference POSC/EEA-ESE/57708/2004 entitled “Fast and accurate power quality measurements using analog to digital converters and digital signal processing techniques”.

REFERENCES

[1] Roger C. Dugan, Mark F. McGranaghan, Surya Santoso, H. Wayne Beaty, *Electrical Power Systems Quality*, 2nd ed., McGraw-Hill, 2002.

[2] L. Cristaldi, A. Ferrero, M. Lazzaroni and R. Ottoboni, “A Linearization Method for Comercial Hall Efect Current Transducers”, *IEEE Trans. on Instrum. Meas,* Vol. 50, No. 5, pp. 1149-1153, Oct. 2001.

[3] Datasheet, “Current Transducer LA 25-NP”, LEM Corporation, available at http://www.lem.com.

[4] Datasheet, “Voltage Transducer LV 25-P”, LEM Corporation, available at http://www.lem.com.

[5] Nuno B. Brás, Pedro M. Ramos and A. Cruz Serra, “Flexible PC measurement system based in Extensible Mark-up Language files”, *14th IMEKO Symposium on New Technologies in Measurement and Instrumentation,* Gdynia, Poland, vol. II, pp. 404-407, Sept. 2005.

[6] *Standard for digitizing waveform records*, IEEE Std. 1057-1994, December 1994.

[7] W. H. Beyer, *CRC Standard Mathematical Tables*, 28th ed. Boca Raton, FL: CRC Press, 1987.